

ORIGINAL ARTICLE

In vivo prostate cancer detection and grading using restriction spectrum imaging-MRI

KC McCammack¹, CJ Kane^{2,7}, JK Parsons^{2,7}, NS White¹, NM Schenker-Ahmed¹, JM Kuperman¹, H Bartsch¹, RS Desikan¹, RA Rakow-Penner¹, D Adams³, MA Liss⁴, RF Mattrey¹, WG Bradley¹, DJA Margolis⁵, SS Raman⁵, A Shabaik³, AM Dale^{1,6} and DS Karow¹

BACKGROUND: Magnetic resonance imaging (MRI) is emerging as a robust, noninvasive method for detecting and characterizing prostate cancer (PCa), but limitations remain in its ability to distinguish cancerous from non-cancerous tissue. We evaluated the performance of a novel MRI technique, restriction spectrum imaging (RSI-MRI), to quantitatively detect and grade PCa compared with current standard-of-care MRI.

METHODS: In a retrospective evaluation of 33 patients with biopsy-proven PCa who underwent RSI-MRI and standard MRI before radical prostatectomy, receiver-operating characteristic (ROC) curves were performed for RSI-MRI and each quantitative MRI term, with area under the ROC curve (AUC) used to compare each term's ability to differentiate between PCa and normal prostate. Spearman rank-order correlations were performed to assess each term's ability to predict PCa grade in the radical prostatectomy specimens.

RESULTS: RSI-MRI demonstrated superior differentiation of PCa from normal tissue, with AUC of 0.94 and 0.85 for RSI-MRI and conventional diffusion MRI, respectively ($P=0.04$). RSI-MRI also demonstrated superior performance in predicting PCa aggressiveness, with Spearman rank-order correlation coefficients of 0.53 ($P=0.002$) and -0.42 ($P=0.01$) for RSI-MRI and conventional diffusion MRI, respectively, with tumor grade.

CONCLUSIONS: RSI-MRI significantly improves upon current noninvasive PCa imaging and may potentially enhance its diagnosis and characterization.

Prostate Cancer and Prostatic Diseases (2016) **19**, 168–173; doi:10.1038/pcan.2015.61; published online 12 January 2016

INTRODUCTION

Radiographic visualization of prostate tumors remains imperfect. Therefore, unlike other solid organ malignancies, definitive diagnosis still relies on systematic biopsy sampling of the entire gland, a procedure that carries risks of pain, bleeding and infection.^{1,2} Improved imaging techniques that reliably detect prostate cancer (PCa) would allow for enhanced diagnosis, targeted prostate biopsies and improved clinical care.

Magnetic resonance imaging (MRI) demonstrates promise for PCa detection, staging and assessing disease aggressiveness. A multiparametric (MP) approach to MRI—consisting of diffusion-weighted imaging (DWI), dynamic contrast enhancement (DCE) and standard anatomic sequencing (T1/T2)—has produced the most reproducible results to date and serves as the standard of care for prostate imaging.^{3–6} MP-MRI fused with ultrasound for targeting prostate biopsy preferentially detects high-grade PCa while minimizing the detection of low-risk disease.^{7,8} These important data suggest targeted biopsy may represent the future standard of care for PCa diagnosis. However, data indicate that targeted biopsy relying on current standard of care prostate MRI fails to detect clinically significant PCa in a substantial number of cases.^{7,8} Continued improvement of prostate MRI is necessary before the widespread acceptance of targeted techniques is achievable.

Restriction spectrum imaging-MRI (RSI-MRI) is a novel, advanced diffusion sequence designed to improve upon the strengths of conventional MRI while correcting its weaknesses. The goal of RSI-MRI is improved conspicuity of highly cellular tumors.^{9–12} It is a multiple b -value, multidirectional diffusion technique, which—via modeling of water compartments in tissue made possible by obtaining an extended spectrum of diffusion images—theoretically focuses observed signals from intracellular, restricted water molecules of interest and attenuates signals from other water molecules that typically confound conventional DWI of the prostate.^{9,10} By focusing on signal arising from intracellular water, the technique in effect images cellularity; highly cellular tumors are thus highlighted by this method. In addition, RSI-MRI corrects the often considerable distortion observed with conventional DWI methods, beneficial in the identification of tumor extension beyond the confines of the prostate.^{9,13}

We hypothesized that RSI-MRI may be a more robust technique for detecting and assessing the aggressiveness of PCa than conventional MP-MRI. In a prior report, we suggested improved characterization of PCa aggressiveness by RSI-MRI.¹⁴ In this study, our primary aim was rather to assess the ability of RSI-MRI compared with conventional MP-MRI to quantitatively differentiate between tumor and normal tissue. A secondary aim of the study was to again assess the ability of RSI-MRI to describe PCa

¹Department of Radiology, University of California San Diego School of Medicine, San Diego, CA, USA; ²Department of Urology, University of California San Diego School of Medicine, San Diego, CA, USA; ³Department of Pathology, University of California San Diego School of Medicine, San Diego, CA, USA; ⁴Department of Urology, University of Texas San Antonio School of Medicine, San Antonio, TX, USA; ⁵Department of Radiology, University of California Los Angeles Geffen School of Medicine, Los Angeles, CA, USA and ⁶Department of Neurosciences, University of California San Diego School of Medicine, San Diego, CA, USA. Correspondence: Dr DS Karow, Department of Radiology, University of California, San Diego, 200 W Arbor Dr, San Diego, CA 92103, USA.

E-mail: dkarow@ucsd.edu

⁷These authors contributed equally to this work.

Received 18 July 2015; revised 19 November 2015; accepted 24 November 2015; published online 12 January 2016

Table 1. MRI sequence acquisition parameters

Sequence	Repetition time (ms)	Echo time (ms)	Field of view (mm)	Matrix	Section thickness (mm)	Flip angle (°)	No. of signals acquired
T2	2567–7367	80–90	200–260	384 × 192	3	90	1
DCE	4.484–4.648	2.1	200	256 × 168	3	30	1
DWI	3750	70.8–74.3	260	160 × 160	5	90	8
RSI ^a	9900	70–72	200–260	96 × 96	3	90	1

Abbreviations: DCE, dynamic contrast enhancement; DWI, diffusion-weighted imaging; MRI, magnetic resonance imaging; RSI, restriction spectrum imaging. ^aRSI-MRI is performed at b -values of 0, 125, 375 and 1000 s mm⁻² with 6, 6 and 15 directions at each respective nonzero b -value.

aggressiveness, but in a completely non-overlapping cohort, without an endorectal coil and on a different imaging platform (GE rather than Siemens) to evaluate generalizability of the technique.

MATERIALS AND METHODS

Patients

The institutional review board approval was obtained for this retrospective study, with signed patient consent waived. Consent was not necessary as RSI-MRI has been integrated into the normal workflow and is performed on all patients undergoing prostate MRI at our institution. All patients who underwent MP-MRI with RSI-MRI performed within 6 months before radical prostatectomy with whole-mount pathology between September 2013 and December 2014 were screened. Required MP-MRI sequences included T1-weighted, T2-weighted, DCE and DWI (including ADC maps). In all, 34 patients fulfilled initial criteria, with one patient excluded from the study due to lack of an available conventional ADC map for the examination.

MRI acquisition

All studies were performed on a 3.0-T GE Signa HDxt scanner (GE Medical Systems, Milwaukee, WI, USA) with a cardiac surface coil but without an endorectal coil. Glucagon was not administered to decrease rectal peristalsis and no bowel preparation was performed. The entire prostate was imaged, with axial slices oriented perpendicular to the rectal wall. The following conventional sequences were obtained: axial and coronal T2-weighted; axial T1-weighted; axial free-breathing DWI (b -values of 0 and 1000 s mm⁻²) and axial free-breathing DCE performed before, during and after single-dose injection of ~20 ml gadobenate dimeglumine (Bracco Imaging, Milan, Italy).

RSI-MRI was performed using spin echo, echo planar imaging at b -values of 0, 125, 375 and 1000 s mm⁻² with 6, 6 and 15 directions at each respective nonzero b -value. The $b=0$ s mm⁻² images were performed with phase encoding in both the forward and reverse directions to correct for spatial distortion due to magnetic field inhomogeneity.¹⁵ Additional specific sequence parameters are summarized in Table 1.

Sample preparation

Whole-mount preparations are performed for all prostatectomies at our institution that have undergone preoperative MRI. After prostatectomy, each specimen was fixed in 10% neutral buffered formalin and then embedded in paraffin. Whole-mount histopathology was performed on 4- μ m-thick sections stained with hematoxylin and eosin. A board-certified anatomic pathologist with over 24 years of experience evaluated the pathology, outlining the boundaries of each tumor and assigning a Gleason score (GS) to each identified tumor.

Histologic–radiologic correlation

Dominant tumors at least 5 mm in diameter as outlined on transverse cut prostate sections by an expert anatomic pathologist (AS; greater than 10 years of specialty experience) were included. The highest GS tumor at least 5 mm in diameter was defined as the dominant tumor. Our pathologist was blinded to imaging results in all cases. For each defined tumor, a corresponding region of interest (ROI) was assigned by an experienced genitourinary radiologist (DK; greater than 3 years of subspecialty experience) on the axial T2-weighted image (Figure 1). In cases where the tumor was not clearly visible on the T2 images, locations were defined as best possible by using anatomic landmarks such as the urethra, ejaculatory ducts and surgical capsule. Each patient had one

tumor ROI included for analysis ($n=33$). In addition to the tumor ROIs, the remaining normal peripheral zone (PZ) was also assigned as an ROI for each patient for comparison, also assigned by the experienced radiologist on the T2 images. These ROIs were then cross-referenced to the respective DCE images, ADC maps and RSI-MRI z-score maps (Figure 1). Two patients had PZ Pca involvement spanning the entirety of the gland, which accounts for the decreased number of control ROIs ($n=31$). Total ROIs ($n=64$) are summarized in Table 2.

Quantitative image analyses

ADC maps were calculated from DWI images at $b=0$ and 1000 s mm⁻² at the scanner console for each voxel of each slice of the prostate. Average voxel values were calculated for each defined ROI and included for analysis.

The Tofts two-compartment model was used in DCE image analysis to calculate the contrast agent transfer rate between blood and tissue (k^{trans}), extravascular extracellular fractional volume (v_e) and contrast backflux rate constant (k_{ep}).¹⁶ Respective maps were calculated using commercial software DynaCAD (Invivo, Gainesville, FL, USA) for each voxel of each slice of the prostate. Average voxel values were calculated for each defined ROI and included for analysis.

RSI-MRI cellularity maps (CMs) were reconstructed using data from all b -values, which were then standardized across all patients to obtain RSI-MRI z-score maps. RSI-MRI z-score maps were calculated by (1) measuring the mean and s.d. of normal prostate signal from the raw RSI-CM data of a representative normal population, (2) subtracting the measured mean value from each subject's CM and (3) dividing the result by the s.d. of measured normal prostate.

PIRADS, a reader-based qualitative standardized reporting system for MP-MRI, was not utilized in this study as this represented a quantitative analysis without reader assessment and scoring. No qualitative reports were used at any point during the study.

Statistical analysis

The ability of each quantitative parameter to differentiate Pca from normal tissue was evaluated using receiver-operating characteristic (ROC) curves, formulated using maximum likelihood estimation. Area under the ROC curve (AUC) analysis was used as a general indicator of quality and was compared statistically between terms using DeLong's test and bootstrapping. RSI-MRI was compared with each individual MP-MRI term even though MP-MRI as a whole serves as the current standard of care, because MP-MRI interpretation of all components is a reader-based qualitative process, whereas this served by design as a quantitative study comparing RSI-MRI with each MP-MRI term objectively. The Spearman rank-order correlation coefficient (ρ) was calculated for each quantitative term to evaluate its strength of association with post-prostatectomy GS. All tests were two-sided, with $P < 0.05$ deemed to reflect statistical significance. All analyses were performed using R version 3.1.2 (The R Foundation for Statistical Computing, Vienna, Austria).

Qualitative analysis

In a subset of the 33 patients in this study, initial tumor was discovered by MR-fused ultrasound-targeted biopsy rather than conventional biopsy. For purposes of showing the qualitative conspicuity of RSI-MRI over conventional DWI and perfusion imaging, tumor ROIs in the biopsy planning software DynaCad, UroNav (Invivo) are shown (Figure 2).

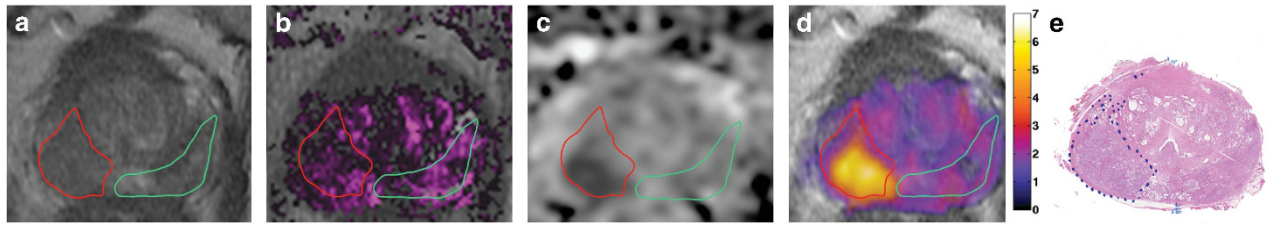


Figure 1. Example tumor (red) and normal peripheral zone (green) region of interest (ROI) assignment to the patient's T2 image (a), subsequently coregistered to the K^{trans} map overlaid on T2 (b), conventional ADC map (c) and restriction spectrum imaging-magnetic resonance imaging (RSI-MRI) map overlaid on T2. The provided RSI-MRI color bar scale demonstrates corresponding z-score (d). ROI definitions were made on T2 images by an experienced radiologist based on the whole-mount hematoxylin and eosin section (e) tumor outlines provided by genitourinary pathology. Final pathology in this case demonstrated Gleason score 4+5=9.

Table 2. Characteristics of tumor and normal PZ ROIs

Characteristic	GS 6	GS 7	GS 8	GS 9	GS 10	All PCa	Normal PZ
No. of ROIs	3	23	3	3	1	33	31
ROI size (mm ²) ^a	72 (83–124)	136 (43–846)	156 (82–260)	532 (88–749)	676	168 (43–846)	224 (46–610)

Abbreviations: GS, Gleason score; PCa, prostate cancer; PZ, peripheral zone; ROI, region of interest. ^aROI size reported as mean values with respective ranges.

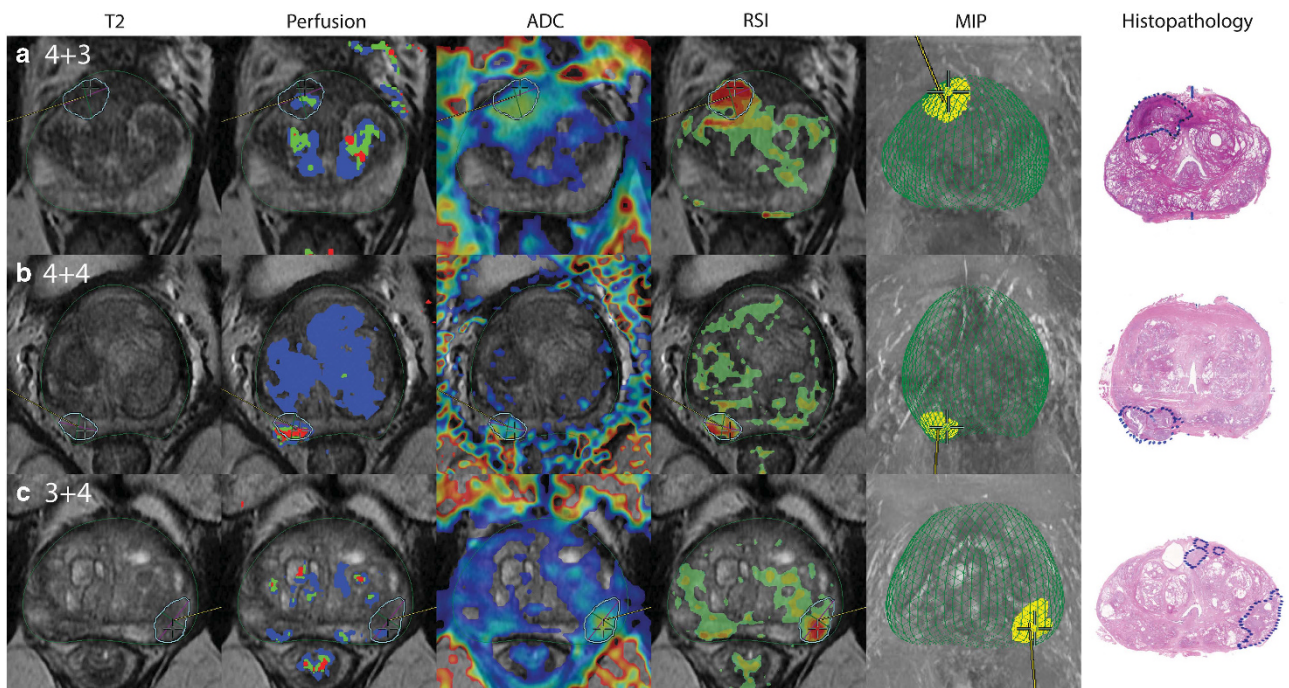


Figure 2. Conventional multiparametric-magnetic resonance imaging components and restriction spectrum imaging-magnetic resonance imaging (RSI-MRI) as used for targeting biopsy. (a) 4+3 Gleason score (GS) prostate cancer (PCa) in the right anterior mid central gland, (b) 4+4 GS PCa in the right posterior base peripheral zone, (c) 3+4 GS PCa in the left posterior mid peripheral zone. In these cases, RSI-MRI more conspicuously demarcates PCa for targeted biopsy than T2, dynamic contrast enhancement or conventional diffusion-weighted imaging techniques as confirmed by post-prostatectomy whole-mount pathology.

RESULTS

Patient characteristics

A total of 33 patients satisfied the inclusion criteria for this study. Mean patient age was 62.5 (range 48–75) years. Mean preoperative PSA concentration was 8.8 (range 1.1–28.0) ng ml⁻¹. Mean time interval between MRI and prostatectomy was 48.9 (range 5–117) days. Pathological disease stage was most commonly pT2c

(N=17), ranging from PT2a to PT3b. Additional patient characteristics are summarized in Table 3.

Discrimination between PCa and normal prostate

We assessed the ability of RSI-MRI to detect PCa tumors relative to conventional DWI and DCE methods. Figure 1 shows a representative case. The tumor ROI (red) and normal ROI (green) were

drawn on the T2-weighted imaging based on histopathology, and transposed to perfusion, ADC and RSI-MRI maps. RSI-MRI z-scores demonstrated the greatest single-term AUC of 0.94. Conventional ADC values demonstrated an AUC of 0.85, statistically inferior performance compared with RSI z-scores ($P=0.04$). RSI-MRI z-scores also outperformed the DCE parameters of K^{trans} ($P=0.03$), k_{ep} ($P=0.007$) and v_e ($P=0.02$). Maximum accuracy for RSI-MRI, ADC and K^{trans} was 87.5%, 79.7% and 78.1%, respectively. The ability of each quantitative term to discriminate between PCa and normal PZ tissue as evaluated by ROC curves is shown in Table 4 and Figure 3.

Correlation with GS

We observed a strong correlation with dominant tumor GS in the radical prostatectomy specimens for RSI-MRI ($\rho=0.53$, $P=0.002$), higher than that seen with conventional diffusion MRI ($\rho=-0.42$, $P=0.01$) and PSA ($\rho=0.36$, $P=0.04$) (Table 5). We found no significant correlation for K^{trans} ($\rho=0.18$, $P=0.30$), k_{ep} ($\rho=0.18$, $P=0.32$) or v_e ($\rho=0.19$, $P=0.30$; Table 5).

DISCUSSION

Compared with conventional MRI, RSI-MRI demonstrated superior accuracy for discriminating between PCa and normal prostate tissue and better correlated with prostatectomy GS. We conclude that RSI-MRI significantly improves upon the clinical performance of conventional MRI for PCa detection, and offers promise as an

improved noninvasive biomarker for PCa grading. Another advantage is that RSI-MRI does not require an endorectal coil.

MRI fused with ultrasound for purposes of PCa-targeted biopsy is currently under investigation. It detects PCa missed by systematic biopsy, provides a greater PCa yield per core and preferentially identifies high-grade PCa.^{7,8,17,18} In addition, it decreases the detection of clinically insignificant PCa.^{7,8} Given these recent data, it appears targeted techniques likely represent the future standard of care. However, a limitation to this transition remains that, as currently practiced, targeted biopsy misses some high-grade, clinically significant PCa, which would be detected by traditional non-targeted systematic biopsy.^{7,8} This is presumably a reflection of the known limitations in the current standard-of-care prostate MRI methodology. Advances in MRI performance likely offer the greatest opportunity to improve targeted biopsy, and RSI-MRI may represent an important step in this effort.

We qualitatively observe greater PCa conspicuity on RSI-MRI compared with standard-of-care MRI regularly and use these data to guide our biopsy targeting efforts more frequently than DCE or conventional DWI (Figure 2). A quantitative validation of this approach is now provided in this study. Specifically, in a group of patients with known PCa, ROC analyses demonstrate that RSI-MRI exhibits greater discrimination accuracy than other parameters included in standard-of-care MRI, with an AUC of 0.94. This figure is admittedly quite high in large part due to study design, which involved placing ROIs for analysis in areas of known PCa as guided by subsequent whole-mount pathology, even when prospective qualitative analysis by a radiologist may not identify disease. However, this is a design with precedent in the literature, which allows direct comparison of quantitative terms in a format impervious to reader error and potential bias, and our results with RSI-MRI are among the most impressive of those studies.^{3,4,19,20} Although not performed at precisely the same b -values as RSI-MRI, conventional ADC values demonstrated reasonable discrimination, with an AUC similar to or better than other published data at 0.85, however this performance is statistically inferior to RSI-MRI.^{3,19,20} Peritumoral edema and necrosis may negatively affect the ability of conventional DWI to localize PCa, as well as signal heterogeneity within normal prostatic tissue itself, leading to the inferior ROC performance, factors that should not as significantly affect RSI-MRI by design.^{10–12} DCE parameters were also outperformed by RSI-MRI, with AUC figures in agreement with published data.^{3,4} With the superior imaging performance of RSI-MRI, we expect improved targeted biopsy performance relative to prior studies and are currently evaluating our results relative to traditional non-targeted systematic biopsy in both screening and active surveillance populations.

ADC values are predictive of PCa aggressiveness on biopsy or prostatectomy GS.^{21–23} A noninvasive imaging biomarker for disease aggressiveness would be valuable for prognostication. Our data support RSI-MRI as a superior imaging biomarker for PCa grading, outperforming DWI in this patient cohort at identical

Table 3. Comprehensive clinical patient characteristics

Characteristic	Average (range)
Age (years)	62.5 (48–75)
Preoperative PSA (ng ml ⁻¹)	8.8 (1.1–28.0)
Tumor volume (ml)	6.5 (0.3–41.8)
Prostate volume (ml)	45.6 (18.0–153.8)
BMI (kg/m ²)	26.8 (20.7–32.6)
Clinical T stage	Number
T1c	21
T2a	9
T2b	2
T2c	1
Pathological T stage	Number
pT2a	2
pT2c	17
pT3a	12
pT3b	2

Abbreviation: BMI, body mass index.

Table 4. Effectiveness of quantitative imaging features in the differentiation of prostate cancer from normal gland

Test	AUC (%)	P ^a	Maximum accuracy (%)	Cutoff value
RSI z-score	93.6 (87.6–99.7)	1	87.5	0.47
ADC values	84.8 (75.4–94.3)	0.04	79.7	1253 mm ² s ⁻¹
K^{trans}	79.2 (67.7–90.6)	0.03	78.1	0.85 ml g ⁻¹ min ⁻¹
k_{ep}	74.0 (61.6–86.4)	0.007	70.3	3.66 min ⁻¹
v_e	77.9 (66.8–89.1)	0.02	71.9	0.29 ml g ⁻¹

Abbreviation: AUC, area under the receiver-operating characteristic curve; MRI, magnetic resonance imaging; RSI, restriction spectrum imaging. ^aEach P -value compares the individual term AUC to RSI-MRI AUC.

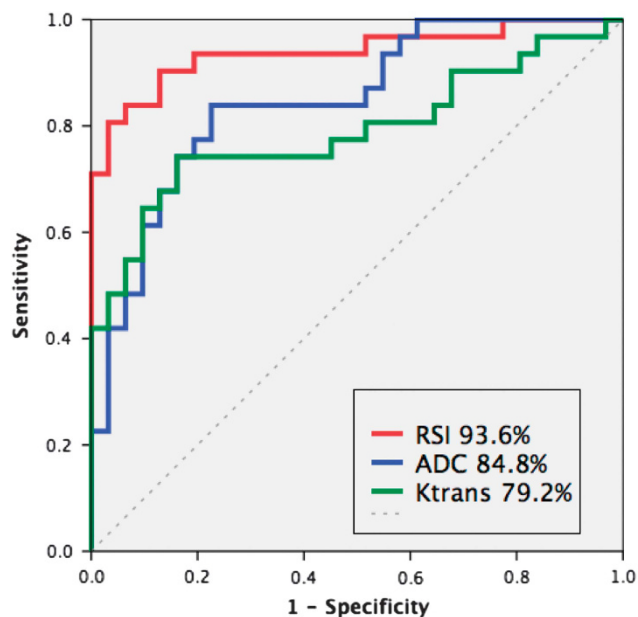


Figure 3. Receiver-operating characteristic (ROC) curves demonstrating performance of restriction spectrum imaging (RSI)-magnetic resonance imaging z-score, conventional ADC values and K^{trans} for the quantitative discrimination of prostate cancer from normal peripheral zone. Respective areas under the ROC curve are listed in the legend.

maximum b -value (Table 3). We have suggested this improved capacity of RSI-MRI over DWI previously, and the current data support that preliminary conclusion using data acquired on a different imaging platform (GE rather than Siemens), as well as without an endorectal coil.¹⁴ These data support the performance of RSI-MRI as generalizable across different platforms and additionally addresses quantitative PCa discrimination by RSI-MRI, which we have not previously investigated in any population.

Equally important as improved PCa conspicuity is accuracy of tumor localization, with image distortion a particularly problematic challenge encountered with conventional DWI.¹⁵ RSI-MRI employs spatial distortion correction using opposed phase-encoding polarities, allowing for efficient anatomic localization, an advance that has demonstrated promise for improved preoperative determination of extraprostatic extension of disease.^{9,13,15,24} Although not specifically examined in this work, this spatial distortion correction may allow the use of the superior tumor conspicuity available with RSI-MRI for accurate targeted biopsy and/or treatment strategies, and these are currently under investigation by our group.

Finally, given the success of RSI-MRI for noninvasive tumor detection in the brain and now prostate, we are optimistic that this technique will be generalizable for the detection of other solid organ tumors. Recent work shows that two-thirds of cancers have no genetic or environmental predisposition.²⁵ This highlights the importance of noninvasive screening measures that can be performed rapidly and inexpensively. RSI-MRI can be performed in 5 min, does not require intravenous contrast and is non-radiation-based. A noninvasive imaging technique that can accurately detect, localize and grade tumors will serve an important diagnostic role but also may serve to guide biopsies and interventions. Further work will assess whether RSI-MRI is a useful biomarker for additional solid organ tumors.

One potential limitation of this study is the relatively small sample size. However, every patient had a prostatectomy sample available for comparison, and utilizing prostatectomy as the gold standard avoided the inaccuracies associated with systematic

Table 5. Spearman rank-order correlation with post-prostatectomy GS results

Test	ρ	P
RSI z-score	0.53	0.002
ADC values	-0.42	0.01
PSA	0.36	0.04
K^{trans}	0.18	0.30
k_{ep}	0.18	0.32
V_e	0.19	0.30

Abbreviations: GS, Gleason score; RSI, restriction spectrum imaging.

biopsy results.^{26–28} A second potential limitation is that we compared PCa tumor ROIs only with normal PZ ROIs in this study. Central gland imaging is a known challenge with regards to PCa however, due to the known predominance of PCa in the PZ, we opted to focus on this location for the quantitative evaluation of RSI-MRI performance in the prostate.^{29–31} In addition, most previously published quantitative studies focus on comparison with the normal PZ as well.^{3,6,19,20} With increased sample size, dedicated central gland performance evaluation will be appropriate and we suspect RSI-MRI will lend itself particularly well in this effort due to its decreased vulnerability to background tissue heterogeneity resulting from the focus on signal arising from within individual cells. Third, the retrospective study design serves as a potential limitation. As a result of this design, some variation in time interval between imaging and prostatectomy is to be expected, which could conceivably be minimized in a prospective study design. Given the indolent progression of PCa, this is likely of minimal impact, if any. In addition, utilizing retrospective assignment of ROIs based on whole-mount pathology does not fully support the improved clinical utility of RSI-MRI over MP-MRI, and prospective reader-based blinded data evaluating this will be needed to evaluate for true clinical utility.

In summary, RSI-MRI shows promise as a noninvasive imaging PCa biomarker, with improved PCa discrimination relative to current standard-of-care conventional MRI terms, as well as more accurate assessment of disease aggressiveness. Our work additionally suggests that RSI-MRI, with its increased accuracy and characterization capabilities, may enable further optimization of image-guided biopsies.

CONFLICT OF INTEREST

The authors declare no conflict of interest.

ACKNOWLEDGEMENTS

This study was funded by grant R01EB000790; American Cancer Society, Institutional Research Grant Number 70-002; DoD, Prostate Cancer Research Program, Idea Development Award W81XWH-13-1-0391, #PC120532; National Science Foundation, Grant Number 1430082; UCSD Clinician Scientist Program; and General Electric, Investigator-Initiated Research Award BOK92325.

REFERENCES

- 1 Chou R, Crosswell JM, Dana T, Bougatsos C, Blazina I, Fu R et al. Screening for prostate cancer: a review of the evidence for the U.S. Preventive Services Task Force. *Ann Intern Med* 2011; **155**: 762–771.
- 2 Moyer VA. Screening for prostate cancer: US Preventive Services Task Force recommendation statement. *Ann Intern Med* 2014; **157**: 120–134.
- 3 Langer DL, van der Kwast TH, Evans AJ, Trachtenberg J, Wilson BC, Haider MA. Prostate cancer detection with multi-parametric MRI: logistic regression analysis of quantitative T2, diffusion-weighted imaging, and dynamic contrast-enhanced MRI. *J Magn Reson Imaging* 2009; **30**: 327–334.
- 4 Engelbrecht M, Huisman H, Laheij R, Jager G, van Leenders G, Hulsbergen-Van De Kaa C et al. Discrimination of prostate cancer from normal

- peripheral zone and central gland tissue by using dynamic contrast-enhanced MR imaging. *Radiology* 2003; **229**: 248–254.
- 5 Kozlowski P, Chang SD, Jones EC, Berean KW, Chen H, Goldenberg SL. Combined diffusion-weighted and dynamic contrast-enhanced MRI for prostate cancer diagnosis—correlation with biopsy and histopathology. *J Magn Reson Imaging* 2006; **24**: 108–113.
 - 6 Turkbey B, Pinto PA, Mani H, Bernardo M, Pang Y, McKinney YL *et al*. Prostate cancer: value of multiparametric MR imaging at 3T for detection—histopathologic correlation. *Radiology* 2010; **255**: 89–99.
 - 7 Siddiqui MM, Rais-Bahrami S, Truong H, Stamatakis L, Vourganti S, Nix J *et al*. Magnetic resonance imaging/ultrasound-fusion biopsy significantly upgrades prostate cancer versus systematic 12-core transrectal ultrasound biopsy. *Eur Urol* 2013; **64**: 713–719.
 - 8 Siddiqui MM, Rais-Bahrami S, Turkbey B, George AK, Rothwax J, Shakir N *et al*. Comparison of MR/ultrasound fusion-guided biopsy with ultrasound-guided biopsy for the diagnosis of prostate cancer. *JAMA* 2015; **313**: 390–397.
 - 9 White NS, McDonald CR, Farid N, Kuperman J, Karow D, Schenker-Ahmed NM *et al*. Diffusion-weighted imaging in cancer: physical foundations and applications of restriction spectrum imaging. *Cancer Res* 2014; **74**: 4638–4652.
 - 10 White NS, Leergaard TB, D'Arceuil H, Bjaalie JG, Dale AM. Probing tissue microstructure with restriction spectrum imaging: Histological and theoretical validation. *Hum Brain Mapp* 2013; **34**: 327–346.
 - 11 Kothari P, White N, Farid N, Chung R, Kuperman J, Girard H *et al*. Longitudinal restriction spectrum imaging is resistant to pseudoresponse in patients with high-grade gliomas treated with bevacizumab. *AJNR Am J Neuroradiol* 2013; **34**: 1752–1757.
 - 12 White N, McDonald C, Farid N, Kuperman J, Kesari S, Dale A. Improved conspicuity and delineation of high-grade primary and metastatic brain tumors using “restriction spectrum imaging”: quantitative comparison with high B-value DWI and ADC. *AJNR Am J Neuroradiol* 2013; **34**: 958–964.
 - 13 Rakow-Penner R, White N, Parsons J, Choi H, Liss M, Kuperman J *et al*. Novel technique for characterizing prostate cancer utilizing MRI restriction spectrum imaging: proof of principle and initial clinical experience with extraprostatic extension. *Prostate Cancer Prostatic Dis* 2015; **18**: 81–85.
 - 14 Liss MA, White NS, Parsons JK, Schenker-Ahmed NM, Rakow-Penner R, Kuperman JM *et al*. MRI-derived restriction spectrum imaging cellularity index is associated with high grade prostate cancer on radical prostatectomy specimens. *Front Oncol* 2015; **5**: 1–8.
 - 15 Holland D, Kuperman JM, Dale AM. Efficient correction of inhomogeneous static magnetic field-induced distortion in Echo Planar Imaging. *Neuroimage* 2010; **50**: 175–183.
 - 16 Tofts P, Brix G, Buckley DL, Evelhock JL, Henderson E, Knopp MV *et al*. Estimating kinetic parameters from dynamic contrast-enhanced T1-weighted MRI of a diffusible tracer: standardized quantities and symbols. *J Magn Reson Imaging* 1999; **10**: 223–232.
 - 17 Vourganti S, Rastinehad A, Yerram NK, Nix J, Volkin D, Hoang A *et al*. Multiparametric magnetic resonance imaging and ultrasound fusion biopsy detect prostate cancer in patients with prior negative transrectal ultrasound biopsies. *J Urol* 2012; **188**: 2152–2157.
 - 18 Sonn G a, Chang E, Natarajan S, Margolis DJ, Macairan M, Lieu P *et al*. Value of targeted prostate biopsy using magnetic resonance-ultrasound fusion in men with prior negative biopsy and elevated prostate-specific antigen. *Eur Urol* 2014; **65**: 809–815.
 - 19 Peng Y, Jiang Y, Yang C, Brown J, Antic T, Sethi I *et al*. Quantitative analysis of multiparametric prostate MR images: differentiation between prostate cancer and normal tissue and correlation with Gleason score—a computer-aided diagnosis development study. *Radiology* 2013; **267**: 787–796.
 - 20 Peng Y, Jiang Y, Antic T, Giger M, Eggen S, Oto A. Validation of quantitative analysis of multiparametric prostate MR images for prostate cancer detection and aggressiveness assessment: a cross-imager study. *Radiology* 2014; **271**: 461–471.
 - 21 Oto A, Yang C, Kayhan A, Tretiakova M, Antic T, Schmid-Tannwald C *et al*. Diffusion-weighted and dynamic contrast-enhanced MRI of prostate cancer: correlation of quantitative MR parameters with Gleason score and tumor angiogenesis. *AJR Am J Roentgenol* 2011; **197**: 1382–1390.
 - 22 Nagarajan R, Margolis D, Raman S, Sheng K, King C, Reiter R *et al*. Correlation of Gleason scores with diffusion-weighted imaging findings of prostate cancer. *Adv Urol* 2012; **2012**: 1–5.
 - 23 Bittencourt LK, Barentsz JO, de Miranda LC, Gasparetto EL. Prostate MRI: diffusion-weighted imaging at 1.5T correlates better with prostatectomy Gleason Grades than TRUS-guided biopsies in peripheral zone tumours. *Eur Radiol* 2012; **22**: 468–475.
 - 24 Rakow-Penner RA, White NS, Margolis DJ, Parsons JK, Schenker-Ahmed N, Kuperman JM *et al*. Prostate diffusion imaging with distortion correction. *Magn Reson Imaging* 2015; **33**: 1178–1181.
 - 25 Tomasetti C, Vogelstein B. Variation in cancer risk among tissues can be explained by the number of stem cell divisions. *Science* 2014; **347**: 78–81.
 - 26 Cohen MS, Hanley RS, Kurteva T, Ruthazer R, Silverman ML, Sorcini A *et al*. Comparing the Gleason prostate biopsy and Gleason prostatectomy grading system: the Lahey Clinic Medical Center experience and an international meta-analysis. *Eur Urol* 2008; **54**: 371–381.
 - 27 Kvåle R, Møller B, Wahlqvist R, Fosså SD, Berner A, Busch C *et al*. Concordance between Gleason scores of needle biopsies and radical prostatectomy specimens: a population-based study. *BJU Int* 2009; **103**: 1647–1654.
 - 28 Rajinikanth A, Manoharan M, Soloway CT, Civantos FJ, Soloway MS. Trends in Gleason score: concordance between biopsy and prostatectomy over 15 years. *Urology* 2008; **72**: 177–182.
 - 29 Oto A, Kayhan A, Jiang Y, Tretiakova M, Yang C, Antic T *et al*. Prostate cancer: differentiation of central gland cancer from benign prostatic hyperplasia by using diffusion-weighted and dynamic contrast-enhanced MR imaging. *Radiology* 2010; **257**: 715–723.
 - 30 Akin O, Sala E, Moskowitz CS, Kuroiwa K, Ishill NM, Pucar D *et al*. Transition zone prostate cancers: features, detection, localization, and staging at endorectal MR imaging. *Radiology* 2006; **239**: 784–792.
 - 31 Li H, Sugimura K, Kaji Y, Kitamura Y, Fujii M, Hara I *et al*. Conventional MRI capabilities in the diagnosis of prostate cancer in the transition zone. *AJR Am J Roentgenol* 2006; **186**: 729–742.